JOURNAL OF SOLID STATE CHEMISTRY 22, 179–184 (1977)

Magnetic Properties and Magnetic Structures of CeAl and $PrAl_a$ (PrAl Annealed)

H. ASMAT, B. BARBARA, AND D. GIGNOUX

Laboratoire de Magnétisme, C.N.R.S., 166X, 38042 Grenoble Cedex, France

Received March 24, 1977

The intermetallic compounds CeAl and $PrAl_a$ (PrAl annealed) crystallize in the *Cmcm* orthorhombic space group. They exhibit a metamagnetic behavior below their Néel temperatures. Both compounds have the same noncollinear magnetic structure; rare earth atoms are divided into two sublattices with different magnetization axes which make the same angle with the *b* axis. Inside each sublattice the arrangement of the moments is collinear and antiferromagnetic. We show that the two moment directions are essentially due to the crystal field effects which act on the rare earth ions lying in a low symmetry site.

Introduction

The RAl compounds crystallize in the CeAl-type structure with La, Ce, and Pr, and the DyAl-type structure for the rare earths going from Pr to Tm (*1*). PrAl crystallizes in the DyAl type when it is quenched from the melting point ($PrAl_q$) and in the CeAl type after annealing ($PrAl_a$). The magnetic properties and the magnetic structures of NdAl, TbAl, HoAl, ErAl, and TmAl have been studied previously by Bècle *et al.* (*2*). In the four non-collinear-type structures observed the moment directions are closely related to the local surroundings and have been interpreted by studying the crystal field effects acting on the rare earth ions located in a low symmetry site (*3*). In this paper, we present the magnetic properties and structures observed on polycrystalline samples of CeAl and $PrAl_a$.

Experimental

The rare earths and aluminum were, respectively, 99.9 and 99.99% pure. Polycrystalline samples were prepared by melting the constituents in a levitation furnace. In order to get a single phase they were annealed one week at 600°C for CeAl and at 800°C for PrAl. The CeAl-type phase was thus obtained. Magnetic measurements were performed at the "Service National des Champs Intenses" (Grenoble) in fields up to 140 kOe between 4.2 and 300°K. The neutron diffraction experiments were made at the "Laboratoire de Diffraction Neutronique du Centre d'Etudes Nucléaires de Grenoble." The neutron wavelength was 1.15 Å.

Crystallographic Structure

CeAl and $PrAl_a$ crystallize in the *Cmcm* space group. The unit cell parameters are shown in Table I. The crystallographic cell contains eight rare earth atoms in the 8*g* site and eight aluminum atoms in the 4*b* and 4*c*

TABLE I

UNIT CELL PARAMETERS OF CeAl AND $PrAl_a$

Compound	*a* (Å)	*b* (Å)	*c* (Å)
CeAl	9.267	7.680	5.746
$PrAl_a$	9.146	7.625	5.698

ISSN 0022-4596

TABLE II

ATOMIC POSITIONS OF THE RARE EARTH ATOMS FOR CeAl AND $PrAl_a$ WHICH CRYSTALLIZE IN THE *Cmcm* SPACE GROUP

Atom number	x	y	z
1	x	y	$\frac{1}{4}$
2	$x+\frac{1}{2}$	$y+\frac{1}{2}$	$\frac{1}{4}$
3	$\bar{x}$	y	$\frac{1}{4}$
4	$\bar{x}+\frac{1}{2}$	$y+\frac{1}{2}$	$\frac{1}{4}$
5	x	$\bar{y}$	$\frac{3}{4}$
6	$x+\frac{1}{2}$	$\bar{y}+\frac{1}{2}$	$\frac{3}{4}$
7	$\bar{x}$	$\bar{y}$	$\frac{3}{4}$
8	$\bar{x}+\frac{1}{2}$	$\bar{y}+\frac{1}{2}$	$\frac{3}{4}$

sites. The Ce and Pr atoms have the same reduced coordinates ($x = 0.179$ and $y = 0.161$) and their positions are reported in Table II.

The crystallographic structure is formed from aluminum chains and rare earth trigonal prisms similar to a half-cell of CsCl.

Magnetic Properties

Previous magnetic measurements have been performed by Kissel and Wallace (*4*).

CeAl

Above 40°K, the thermal variation of the reciprocal susceptibility is linear with a paramagnetic Curie temperature $\Theta_p = -12$°K (Fig. 1); the effective moment ($2.4 \pm 0.2\ \mu_B$) is close to the free ion one ($2.56\ \mu_B$). Below 40°K the variation is no longer linear and passes through a minimum at 10°K, the Néel temperature of the compound.

The variation of the magnetization with the applied field measured at 4.2°K is shown on Fig. 2. The magnetization, which increases slowly and linearly in low field, exhibits two transitions, respectively, at 5.5 and 14 kOe. In higher fields the magnetization tends to saturate. However, in 150 kOe, the magnetization is only $1.8\ \mu_B$/Ce. A similar behavior is observed at all temperatures below T_N.

PrAl

As for CeAl, above 50°K the thermal variation of the susceptibility follows a Curie–Weiss law with a paramagnetic Curie temperature of $\Theta_p = -4$°K (Fig. 1). The effective moment ($3.4 \pm 0.2\ \mu_B$) is in agreement with that of the free ion Pr^{3+} ($3.52\ \mu_B$). The susceptibility exhibits a maximum at 18°K, the Néel temperature of the compound. Below the Néel temperature two transitions with a small hysteresis are observed at 21.5 and 72 kOe (Fig. 2). In 150 kOe, the magnetization is only $1.25\ \mu_B$/Pr.

Magnetic Structures

CeAl

The neutron diffraction patterns performed on a polycrystalline sample of CeAl at 77 and

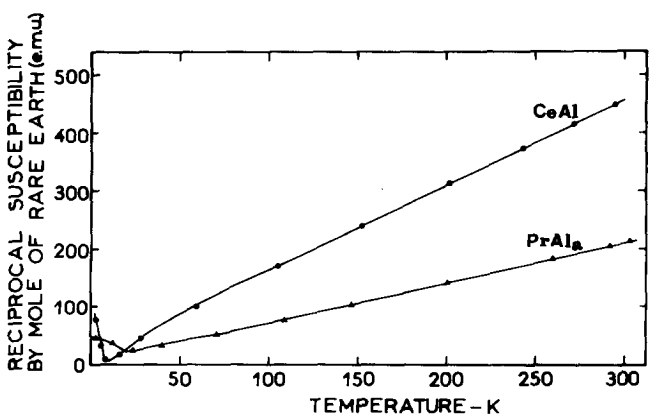

FIG. 1. Thermal variation of the reciprocal susceptibility of CeAl and $PrAl_a$.

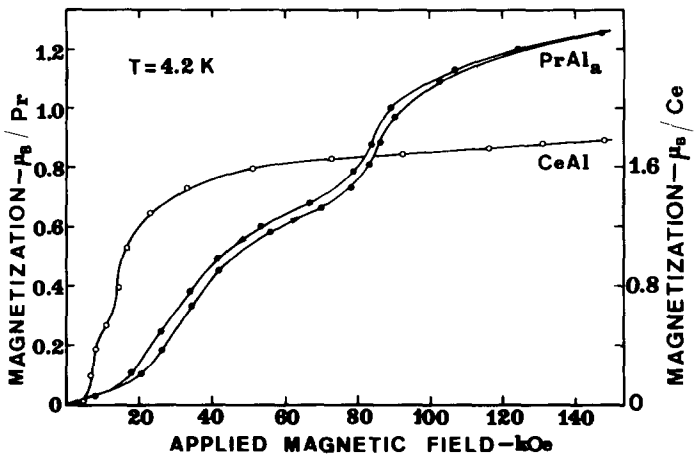

FIG. 2. Variation of magnetization of polycrystalline samples of CeAl and $PrAl_2$ at 4.2°K.

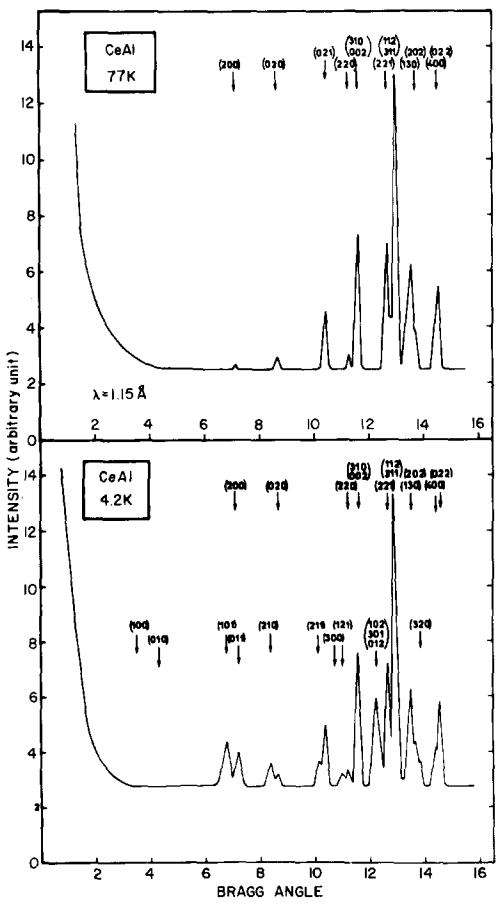

FIG. 3. CeAl: neutron diffraction patterns at 77 and 4.2°K.

4.2°K are shown in Fig. 3. At 77°K the intensities of the peaks are characteristic of the crystallographic structure (Table IV). In particular, because of the translation $[\frac{1}{2}, \frac{1}{2}, 0]$, the (hkl) reflections with $h + k = 2n + 1$ do not appear. At 4.2°K, new peaks appear. They are indexed in the crystallographic cell ($\tau = 0$) with $h + k = 2n + 1$. No magnetic contributions appear for the nuclear reflections. The translation $[\frac{1}{2}, \frac{1}{2}, 0]$ no longer exists. The moments of the rare earth atoms 1, 3, 5, and 7 are, respectively, antiparallel to those of the atoms 2, 4, 6, and 8.

In order to interpret this pattern we have used the "Macroscopic method" developed by Bertaut (*5*). There are eight irreducible representations associated with the propagation vector $\tau = 0$ of the crystallographic group; they are real and have one dimension. The basis vectors associated with each representation are defined from the component of the classical vectors **F**, **G**, **C**, and **A** which are linear combinations of the spins of the atoms 1, 3, 5, and 7. These basis vectors are obtained by means of the projection operator method and are reported in Table III.

The calculation of the structure factors associated with the four basis vectors for the different reflections (hkl) has allowed us to select the modes describing the magnetic structure.

TABLE III

Cmcm GROUP ASSOCIATED WITH THE PROPAGATION VECTOR $\tau = 0$: IRREDUCIBLE REPRESENTATIONS AND BASIS VECTORS[a]

Irreducible representations	Symmetry elements								Basis vectors		
	E	2_x	2_y	2_{1z}	1	m_x	C	m_z			
Γ_1	1	1	1	1	1	1	1	1	—	—	A_z
Γ_2	1	−1	1	−1	1	−1	1	−1	A_x	F_y	—
Γ_3	1	1	−1	−1	1	1	−1	−1	F_x	A_y	—
Γ_4	1	−1	−1	1	1	−1	−1	1	—	—	F_z
Γ_5	1	1	1	1	−1	−1	−1	−1	G_x	C_y	—
Γ_6	1	−1	1	−1	1	−1	1	−1	—	—	G_z
Γ_7	1	1	−1	−1	−1	−1	1	1	—	—	C_z
Γ_8	1	−1	−1	1	−1	1	1	−1	C_x	G_y	—

[a] The basis vectors are the following linear combinations of the spin 1, 3, 5, and 7: $F = (++++)$, $G = (+-+-)$, $C = (++--)$, $A = (+--+)$.

The observed diffraction pattern can only be interpreted with the antiferromagnetic modes G_x and C_y which belong to the Γ_5 representation. In Table IV we have compared the observed and calculated intensities ($R = \sum |I_o - I_c| / \sum I_c = 6.6\%$). The magnetic structure is noncollinear; cerium atoms can be divided into two sublattices with different magnetization axes which make the same angle, Ψ, with the b axis (Fig. 4). Inside each sublattice the arrangement of the moments is collinear and antiferromagnetic. The magnetic structure belongs to the magnetic space group $Pm'c'm'$.

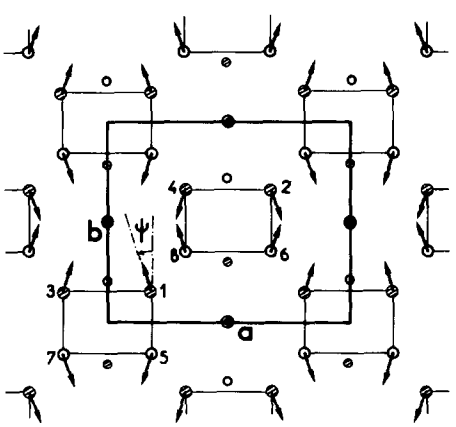

FIG. 4. Magnetic structure of CeAl and $PrAl_a$; the moments lie in the (a, b) plane.

The values of the cerium moment and of the Ψ angle are reported in Table V.

$PrAl_a$

The neutron diffraction pattern performed at 4.2°K on a polycrystalline sample is identical to that of CeAl and corresponds to the same magnetic structure. The values of the praseodymium moment and of the Ψ angle are reported in Table V.

Discussion

The interpretation of the noncollinear magnetic structures of CeAl and $PrAl_a$ is analogous to that of the other RAl compounds (*3*) and that of the RNi compounds (*6*). These structures result from the crystal field effects on the rare earth ions which lie in a low symmetry site m (Cs).

The crystal field Hamiltonian can be written using the Stevens equivalent operators:

$$\mathcal{H}_c = \alpha(V_2^0 O_2^0 + V_2^{-2} O_2^{-2} + V_2^2 O_2^2) + \mathcal{H}_4 + \mathcal{H}_6$$

The reference axes are defined in Fig. 5.

In the point charge approximation we have calculated the V_l^m parameters for the R^{3+} ion in position (1). We have assumed a charge +3e for R^{3+} ions and a zero charge on

TABLE IV

CeAl: OBSERVED AND CALCULATED NEUTRON DIFFRACTION INTENSITIES AT 77 AND 4.2°K

$h\,k\,l$ $(h+k=2n)$	θ	$I_{N,\mathrm{cal}}$	$I_{N,\mathrm{obs}}$
1 1 0	5.58	0.11	n.o.
0 0 1	5.75	0.0	n.o.
2 0 0	7.13	0.28	n.o.
1 1 1	8.02	0.02	n.o.
0 2 0	8.61	4.45	n.o.
2 0 1	9.17	0.0	n.o.
0 2 1	10.46	30.14	26.44
2 2 0	11.21	5.80	n.o.
0 0 2	11.64	63.65	63.88
3 1 0	11.72		
2 2 1	12.75	61.47	63.06
1 1 2	12.97	206.74	209.90
3 1 1	13.11		
1 3 0	13.58	82.03	88.50
2 0 2	13.76		
4 0 0	14.56	75.55	67.80
0 2 2	14.59		

$h\,k\,l$ $(h+k)=2n+1$	θ	$I_{M,\mathrm{cal}}$	$I_{M,\mathrm{obs}}$
1 0 0	3.56	0.0	n.o.
0 1 0	4.29	0.0	n.o.
1 0 1	6.76	11.98	12.80
0 1 1	7.18	11.34	9.74
2 1 0	8.33	8.70	8.20
1 2 0	9.33	0.0	n.o.
2 1 1	10.14	16.19	14.86
3 0 0	10.73	0.0	n.o.
1 2 1	10.98	9.91	10.60
1 0 2	12.09		
3 0 1	12.20	73.00	76.95
0 1 2	12.34		
0 3 0	12.98	0.0	n.o.

aluminum. This calculation shows that the second-order terms play a preponderant role in $\mathscr{H}_a$. As proposed by Rossat-Mignod and

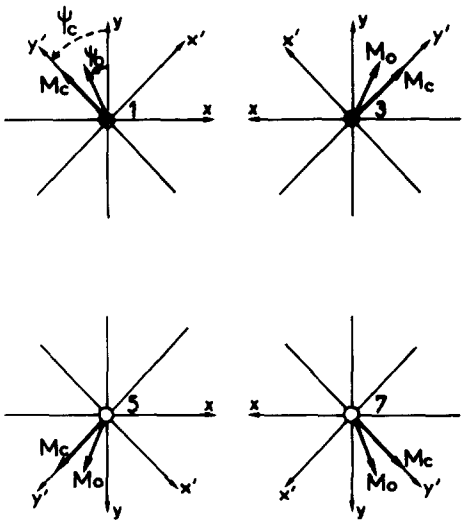

FIG. 5. Reference axes before and after rotation in each position of the rare earth site deduced by symmetry operations.

Tchéou (7), by a rotation around the Oz axis with angle Ψ_c such as $tg\,2\Psi_c = V_2^{-2}/V_2^2$, it is possible to get a D_2-like symmetry in the Hamiltonian. The calculated Ψ_c angles are the same (45°) for CeAl and $PrAl_a$. In this new symmetry we can then calculate the ground state multiplet splitting and show that in this approximation cerium and praseodymium moments have to be parallel to the new Oy' axis. Because of the symmetry elements of the space group the rare earth atoms are then divided into two sublattices with different easy magnetization directions. This accounts for the observed magnetic structure. However, the calculated Ψ_c angle is greater than the observed one, Ψ_0 (Table V) because the calculation neglects the imaginary terms $V_4^{-2}O_4^{-2}$ and $V_4^{-4}O_4^{-4}$ which are not nul.

TABLE V

NÉEL TEMPERATURES AND RARE EARTH MOMENTS FOR CeAl AND $PrAl_a$

Compound	T_N (K)	g_J	M_{obs} (μ_B)	M_{cal} (μ_B)	ψ_{obs}(°)	ψ_{cal} (°)
CeAl	10	2.14	2.1 ± 0.2	2.0	19 ± 2	45
$PrAl_a$	18	3.20	2.9 ± 0.2	2.7	24 ± 2	45

In fact, this method consists of determining the principal axes of the surrounding quadrupole. If we neglect the higher order terms the magnetic moment has to be along one of these principal axes.

In conclusion the noncollinear magnetic structures observed in CeAl and $PrAl_a$ essentially result from a compromise between small isotropic exchange interactions and a strong single ion anisotropy due to the effect of the crystal field on R^{3+} ions.

The two transitions induced by the applied field result from a metamagnetic mechanism. Because of the importance of the anisotropy we can consider that the moments remain almost parallel to the easy magnetization direction (Ising-like model). The first transition corresponds to the appearance of a ferromagnetic component along x; the induced structure belongs to the Γ_3 representation associated with F_x and A_y. At the second transition the structure becomes ferromagnetic along y; this induced structure belongs to the Γ_2 representation associated with A_x and F_y. This second transition occurs in higher fields because the strong induced ferromagnetic component results from a more important competition between the applied field and the negative interactions.

References

1. C. BECLE AND R. LEMAIRE, *Acta Crystallogr.* **23**, 840 (1967).
2. C. BECLE, R. LEMAIRE, AND D. PACCARD, *J. Appl. Phys.* **41**, 855 (1970).
3. J. K. YAKINTHOS AND F. TCHÉOU, *Solid State Commun.* **18**, 1287 (1976).
4. F. KISSEL AND W. E. WALLACE, *J. Less Common Metals* **11**, 417 (1966).
5. E. F. BERTAUT, Magnetism, Rado and Suhl Edt. Vol. **3**, 150–1963).
6. D. GIGNOUX, D. PACCARD, J. ROSSAT-MIGNOD, AND F. TCHÉOU, *in* "Rare Earth Res. Conf., Carefree, Arizona (1973)."
7. J. ROSSAT-MIGNOD AND F. TCHÉOU, *J. Phys.* **33**, 423 (1972).